

Spin dynamics in tunneling decay of a metastable state

Yue Ban¹ and E. Ya. Sherman^{1,2}

¹*Department of Physical Chemistry, The University of the Basque Country UPV/EHU, 48080 Bilbao, Spain*

²*IKERBASQUE Basque Foundation for Science, Bilbao, 48011 Bizkaia, Spain*

(Dated: October 30, 2018)

We analyze spin dynamics in the tunneling decay of a metastable localized state in the presence of spin-orbit coupling. We find that the spin polarization at short time scales is affected by the initial state while at long time scales both the probability- and the spin density exhibit diffraction-in-time phenomenon. We find that in addition to the tunneling time the tunneling in general can be characterized by a new parameter, the tunneling length. Although the tunneling length is independent on the spin-orbit coupling, it can be accessed by the spin rotation measurement.

PACS numbers: 03.65.Xp, 03.75.-b, 71.70.Ej

I. INTRODUCTION

Spin-orbit (SO) coupling, interaction of particle spin or pseudospin with the orbital motion, provides an efficient way to control and manipulate spin, charge, and mass transport. Two different kinds of SO coupled systems attract a great deal of interest due to the known and yet unexplored variety of phenomena they can demonstrate and due to their possible applications in quantum technologies. One class of systems, investigated for more than five decades by now, is semiconductors and semiconductor-based nanostructures [1–7]. The other class, lavished attention only recently, is cold atoms and Bose-Einstein condensates, where by engineering external optical fields one can couple orbital motion to the pseudospin degree of freedom [8–12] and cause Dresselhaus and Rashba types of SO coupling similar to that in solids.

In quantum systems of interest the tunneling plays an important role and either completely determines or strongly influences the particle dynamics. At certain conditions the tunneling rate depends on the spin of the particle [2, 3, 13, 14]. The understanding of the tunneling is the key for the understanding of the transient processes in a broad variety of systems, including, e.g. charge transport in molecular nanostructures [15]. One of the key issues in the tunneling theory is the evaluation of the time spent by the particle in the classically forbidden regions. Similar to the scattering problem of propagating wave packets, the question of the tunneling time for the decay of a metastable system [16–20] may also be posed. The spin-dependent effects based on the Larmor clock concept for potential barriers [21, 22], Hartman effect in graphene [23], and effective exchange fields in semiconductors [24] can provide a measure of this time. In classically forbidden regions there is not only precession but also a rotation of the magnetic moment into the magnetic field direction and the time of the interaction with the barrier is closely related to this rotation [25, 26]. The effects of SO coupling on the tunneling through semiconductor quantum-well structures with a lateral potential barrier [27, 28] provide another tool to utilize electron spin modifying the charge transport in

nonmagnetic systems.

Here we investigate the spin-dependent tunneling of a state initially localized in the potential at short and long compared to the state lifetime time scales [29]. This paper is organized as follows. In Sec. II we introduce the model Hamiltonian and formulate the physical observables of interest. We use the SU(2) spin rotation to gauge out spin-orbit coupling and restore its effects in the calculation of the observables by inverse transformation. In Sec. III we study the dynamics at short time scale, concentrating on spin oscillations, decay, and escape from the localizing potential. In Sec. IV we study long-term dynamics in the far-field zone. The diffraction in time in spin density is observed at a long distance, where SO coupling forms a precursor in the propagating density. We show that the tunneling can be characterized not only by time, but also by a certain length parameter, which can be accessed by detecting the spin precession due to the SO coupling. Conclusions summarize the results.

II. MODEL FOR SPIN-DEPENDENT TUNNELING

As a model we consider shown in Fig.1 time-dependent potential $U(x, t)$, infinite at $x < 0$, with the time-dependence:

$$U(x, t) = U_1(x) \quad (t < 0), \quad U(x, t) = U_2(x) \quad (t > 0). \quad (1)$$

At $t \leq 0$ the potential holds bound states with wave functions $\varphi_j(x)$ and energy E_j ; it changes at $t > 0$ from a step to a barrier to allow the tunneling. Such time-dependent potential can be produced by a recently developed technique [30] where a moving laser beam “paints” a broad variety of coordinate- and time-dependent potentials.

With SO coupling taken into account, the total one-dimensional Hamiltonian is

$$\hat{H} = \frac{1}{2m} \left(\hbar \hat{k}_x + \hat{A}_x \right)^2 + U(x) - \frac{p_{\text{so}}^2}{2m}, \quad (2)$$

with $\hat{k}_x = -i\partial/\partial x$, the vector potential $\hat{A}_x = p_{\text{so}}\hat{\sigma}_x$, $p_{\text{so}} \equiv m\alpha/\hbar$, where α is the Dresselhaus SO coupling

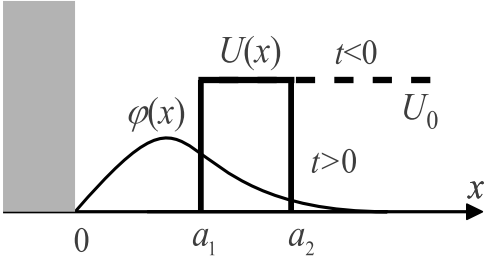


FIG. 1. Time-dependent potential $U(x)$: $U_1(x)$ at $t < 0$ and $U_2(x)$ when $t > 0$. $U_1(x)$ is a step in the positive halfplane, that is zero from $x = 0$ to $x = a_1$ and U_0 from $x = a_1$ to infinity, while $U_2(x)$ is a barrier of the height U_0 extended from $x = a_1$ to $x = a_2$. The potential is always infinite in the negative halfplane. The barrier width is defined as $d \equiv a_2 - a_1$.

constant, and $\hat{\sigma}_x$ is the corresponding Pauli matrix. The spatial scale of spin precession is characterized by the length $2\xi = \hbar/p_{\text{so}}$. The typical values of ξ for different systems with SO coupling can be of interest. For (i) electrons in semiconductor GaAs nanostructures [1] with $m \approx 6 \times 10^{-29}$ g, $\alpha/\hbar \sim 0.5 \times 10^6$ cm/s, (ii) for ${}^6\text{Li}$ atoms [9] with $m \approx 10^{-23}$ g, $\alpha/\hbar \sim 10$ cm/s, and (iii) for ${}^{87}\text{Rb}$ atoms [12] with $m \approx 1.5 \times 10^{-22}$ g, $\alpha/\hbar \sim 0.3$ cm/s, we obtain $\xi \sim 10^{-5}$ cm. It is interesting to mention that although masses and coupling constants for electrons in nanostructures and cold atoms are very different, the resulting precession length is on the same order of magnitude for all these systems. Since typical localization scale of electrons in nanostructures a_1 is on the order of 10^{-6} cm, they are in the weak-coupling regime with $\xi/a_1 \gg 1$. Cold atoms, however, are localized on the scale of the order visible light wavelength, that is of 10^{-4} cm, and the strong SO coupling regime with $\xi < a_1$ can be achieved there. The characteristic timescale corresponding to the particle motion inside the potential, ma_1^2/\hbar , is on the order of 0.1-1 ps for electrons in nanostructures and 0.1-1 ms for cold atoms.

From now on we use the system of units with $\hbar \equiv 1$ and particle effective mass $m \equiv 1$. The wave function corresponding to \hat{H} is $\psi(x, t)$ with the initial state set as

$$\psi(x, 0) = \chi\varphi_j(x), \quad (3)$$

and the spinor $\chi = [1, 0]^T$ corresponds to the z -axis orientation. Such a function can be produced by applying a magnetic field along the z -axis for an electron or by a special design of optical field in the case of a neutral bosonic atom [12]. At $t > 0$, neither the orbital wave function φ_j is the eigenstate, nor χ is the eigenspinor of Hamiltonian \hat{H} . The initial state begins to evolve at $t > 0$ with spin precession and the probability to find the particle inside the potential decreases simultaneously.

We use a gauge transformation $\hat{H} = \mathbf{S}\hat{H}\mathbf{S}^{-1}$ with a unitary matrix $\mathbf{S} = \exp(i\hat{\sigma}_x x/2\xi)$ to gauge away the SO coupling. The gauge transformation shifts \hat{k}_x by $\hat{\sigma}_x/2\xi$

and turns SO coupling into a constant, with the wave function evolving in time transformed as:

$$\tilde{\psi}(x, t) = \mathbf{S}\psi(x, t) = \begin{bmatrix} \tilde{\psi}_1(x, t) \\ \tilde{\psi}_{-1}(x, t) \end{bmatrix}, \quad (4)$$

with the upper and lower components

$$\tilde{\psi}_\sigma(x, t) = \int_0^\infty G_\sigma(k)\phi_k(x) \exp\left(-\frac{ik^2 t}{2}\right) dk, \quad (5)$$

and the coefficients are

$$G_\sigma(k) = \int_0^\infty \tilde{\psi}_\sigma(x, 0)\phi_k(x) dx. \quad (6)$$

Here, $\phi_k(x)$ is the eigenstate of the Hamiltonian corresponding to $U_2(x)$:

$$\phi_k(x) = \begin{cases} C(k) \sin(kx), & (0 < x < a_1) \\ D(k)e^{-\kappa_k x} + F(k)e^{\kappa_k x}, & (a_1 < x < a_2) \\ \sqrt{2/\pi} \sin[kx + \theta(k)], & (x > a_2) \end{cases} \quad (7)$$

normalized as $\langle \phi_{k'} | \phi_k \rangle = \delta(k - k')$. The coefficients $C(k)$, $D(k)$, $F(k)$ and the phase $\theta(k)$ satisfy the boundary conditions of the potential $U_2(x)$, and $\kappa_k = \sqrt{2U_0 - k^2}$. In the tunneling regime $k < \sqrt{2U_0}$, while in the propagating regime $k > \sqrt{2U_0}$, and $i\kappa_k$ is substituted by $q = \sqrt{k^2 - 2U_0}$.

The initial wave function corresponding to Hamiltonian \hat{H} can be expressed as

$$\tilde{\psi}(x, 0) = \varphi_j(x) \begin{bmatrix} \cos(x/2\xi) \\ i \sin(x/2\xi) \end{bmatrix}. \quad (8)$$

The coefficients $G_\sigma(k)$ become

$$G_1(k) = \int_0^\infty \cos(x/2\xi)\varphi_j(x)\phi_k(x) dx, \quad (9)$$

$$G_{-1}(k) = i \int_0^\infty \sin(x/2\xi)\varphi_j(x)\phi_k(x) dx. \quad (10)$$

In what follows, we investigate the particle motion by calculating the physical observables such as probability density, spin density, and spin polarization defined as:

$$\rho(x, t) = \psi^\dagger(x, t)\psi(x, t), \quad (11)$$

$$\sigma_i(x, t) = \psi(x, t)^\dagger \hat{\sigma}_i \psi(x, t), \quad (12)$$

$$p_i(x, t) = \frac{\hat{\sigma}_i(x, t)}{\rho(x, t)}, \quad (13)$$

respectively. As the spin rotates around the effective SO coupling field along the x -direction, the integral of $\sigma_x(x, t)$ -component over the $x > 0$ half axis is conserved. For this reason, we investigate spin density and spin polarization in the more informative y -component.

III. SPIN DYNAMICS AT SHORT TIMES

To address the short-term dynamics on the time less than the lifetime of the initial bound state [29], we study two relevant quantities. First quantity is $\sigma_y(a_2, t)$, the spin density at the exit of the barrier a_2 . The other one, $p_y^{[w]}(t)$, defined as

$$p_y^{[w]}(t) = \frac{\int_0^{a_1} \psi^\dagger(x, t) \sigma_y \psi(x, t) dx}{\int_0^{a_1} \psi^\dagger(x, t) \psi(x, t) dx}, \quad (14)$$

being the spin polarization y component in the potential, represents the integrated spin dynamics inside the potential. The denominator of Eq.(14) is the probability to find the particle inside the potential, which decays to $1/e$ of its initial value at the lifetime of the metastable state.

We consider the evolution of three initial orbital states, as shown in Fig.2 for the spin component at the edge. We choose $U_0 = 16$ so that there are two bound states, the ground state φ_0 and the first excited state φ_1 , and use dimensionless $a_1 \equiv 1$. Here, the initial state has a strong impact on the time-dependent $\sigma_y(a_2, t)$. It is demonstrated in Fig.2 that it takes very short time for $\sigma_y(a_2, t)$ to develop into the minimum from zero, irrespective of the initial state. This behavior is similar to the fast development of a plateau in the outgoing flux after the potential change [29]. However, spin density with φ_1 decays faster than that with φ_0 . The linear combination of these two bound states $\varphi_{\text{com}} = (\varphi_0 + \varphi_1)/\sqrt{2}$ shows strong oscillations due to the interference between them. As both spin density and probability density in the potential decay with time, spin polarization tends to a constant at large time.

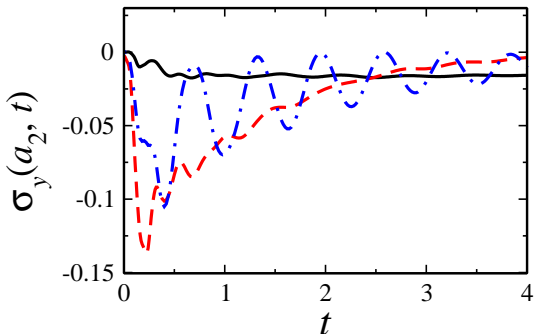


FIG. 2. (Color online) Comparison of time evolution of $\sigma_y(a_2, t)$ at the right edge of the barrier a_2 with different initial states, the ground state φ_0 (solid), the first excited state φ_1 (dashed) and the linear combination $\varphi_{\text{com}} = (\varphi_0 + \varphi_1)/\sqrt{2}$ (dot-dashed), provided by the barrier $d = 0.4$, $U_0 = 16$, and $\xi = 0.5$. Negative $\sigma_y(a_2, t)$ is related to the direction of spin precession determined by the sign of coupling constant α .

The tunneling resulted from various initial states has a strong effect on spin polarization, especially in short-

time scales, as shown in Fig.3. Spin polarization inside the potential oscillates between boundaries. The oscillation rate is fast and determined by the energy difference of the initially bound states. With the time, the contribution of the excited state rapidly decays due to the fast tunneling, and the spin remains in the state achieved by the time of the decay of the upper bound state. The amplitude of resonances for φ_1 is larger than φ_0 , as the former possesses larger momentum. As for the linear combination of these two bound states, the spin polarization is greatly enhanced because of interferences. On the other hand, strength of SO coupling strongly influences the spin polarization in the potential as illustrated by making comparisons for $\xi = 0.5$ and $\xi = 1$ parameters.

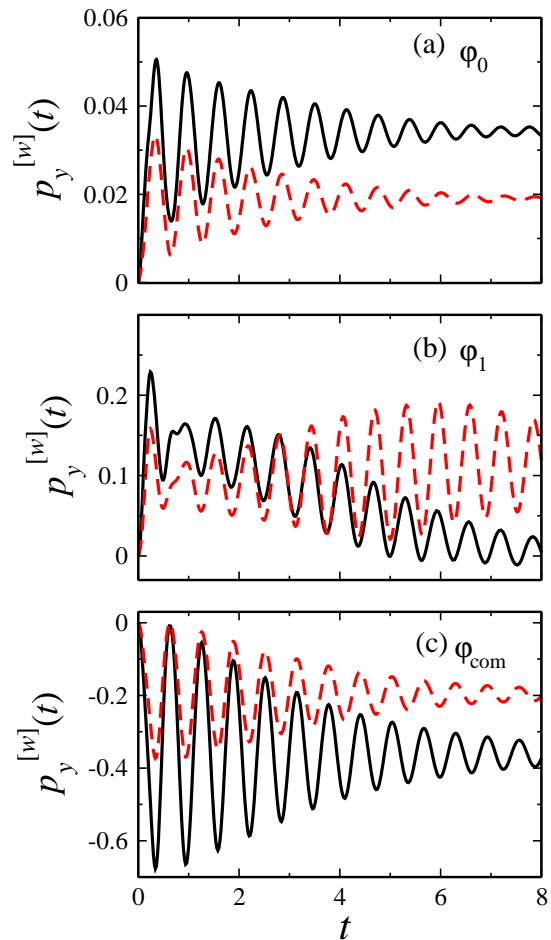


FIG. 3. (Color online) Time evolution of $p_y^{[w]}(t)$ in the potential from 0 to a_1 , caused by SO coupling with $\xi = 0.5$ (solid) and $\xi = 1$ (dashed), with different initial coordinate states: (a) φ_0 , (b) φ_1 , and (c) $\varphi_{\text{com}} = (\varphi_0 + \varphi_1)/\sqrt{2}$, provided by the same barrier as in Fig.2.

Having illustrated the evolution of spin density at the boundary, $\sigma_y(a_2, t)$, and averaged spin polarization, we can address the details of the spin distribution inside the potential. As shown in Fig.4, this distribution oscillates due to the interferences between the ground state and other eigenstates. The amplitude of oscillations becomes

weaker with time as the state decays.

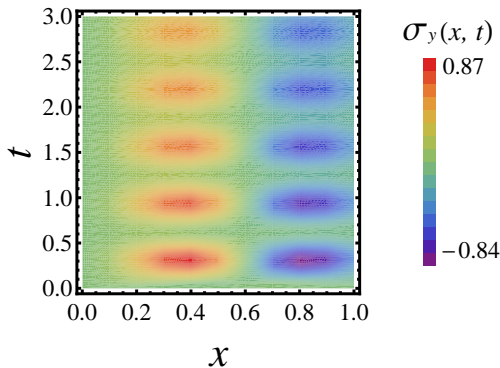


FIG. 4. (Color online) Spin density (y component) in the potential vs time and position for $\xi = 0.5$ and $\psi(x, t = 0) = \chi\varphi_0$. The parameters of the barrier are the same as in Fig.2.

IV. SPIN DYNAMICS IN THE FAR-FIELD ZONE

Here we investigate the long-term spin dynamics, by considering the probability density ρ and y component of spin density $\sigma_y(X, t)$ which can be detected at a given long distance $X \gg 1$. The density evolution for $\rho(X, t)$ at $X = 10\pi$ is shown in Fig.5 for different SO coupling strength. Under different ξ , the time evolutions of probability density show a strong sharp peak followed by oscillations due to the diffraction-in-time process [31–33]. However, unlike the case without SO coupling [29, 34], for strong couplings (small ξ), there exist some oscillations before the sharp peak, where the interference of two velocities of spin up and spin down components are remarkable. A very interesting feature is the precursor of the main peak corresponding to the opposite spin. The precursor becomes stronger with the increase in the SO coupling. The time dependence of $\sigma_y(X, t)$ at $X = 10\pi$ is shown in Fig.6. Different values of ξ result in different spin rotation angles and corresponding spin density, provided that $\sigma_y(x, t)$ is detected at the same position.

Spin precession in the (y, z) -plane is described by the classical precession angle, $\beta_0^{[\text{so}]} = \Omega t$, where the precession frequency is $\Omega \approx 2\alpha k_0 = k_0/\xi$ and the wave packet is detected at the position X at the time instant X/v , the velocity $v = k_0$. Therefore, the rotation angle is $\beta_0^{[\text{so}]} = X/\xi$, independent on time t , provided that the wave packet is considered classically. Ideally, for a free particle propagating from the origin $x(t = 0) = 0$, spin polarizations components are $p_x = 0$, $p_y = -\sin\beta_0^{[\text{so}]}$, $p_z = \cos\beta_0^{[\text{so}]}$. As a result, at $X = n\pi\xi$, the classical spin polarization should be $p_y = 0$. However, in the tunneling problem we consider, the value of p_y is not zero even at $X = n\pi\xi$.

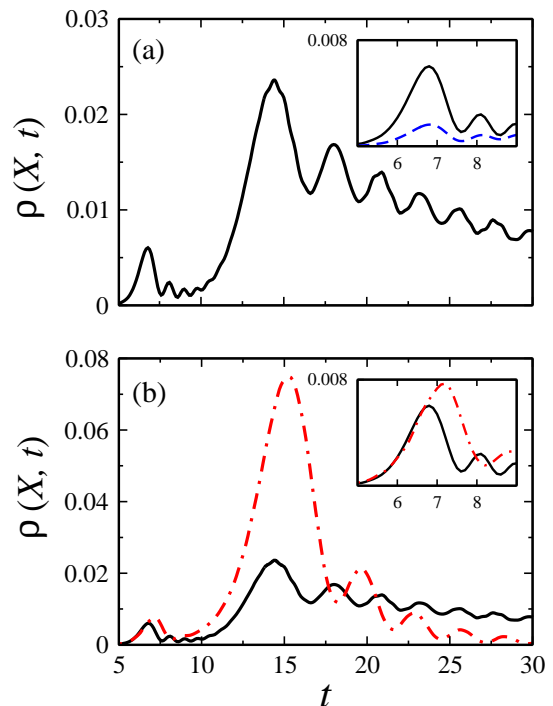


FIG. 5. (Color online) (a) Time-dependent density at the observation point $X = 10\pi$ for system parameter $U_0 = 16$, $d = 0.4$, and $\xi = 0.5$. Inset shows the precursor dynamics on a shorter time scale. Dashed line corresponds to $U_0 = 16$, $d = 0.4$, and $\xi = 1$. (b) Solid line corresponds to $U_0 = 16$, $d = 0.4$, and $\xi = 0.5$, dot-dashed line corresponds to $U_0 = 8$, $d = 0.4$, and $\xi = 0.5$. Inset shows the precursor dynamics on a shorter time scale.

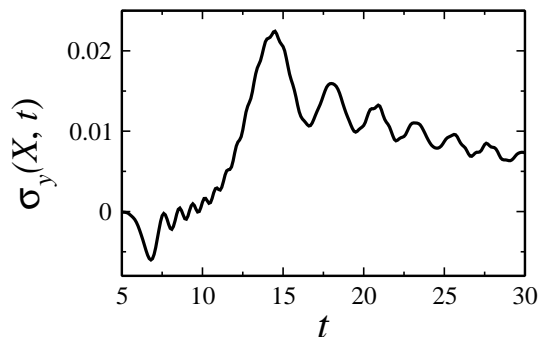


FIG. 6. Spin density in the observation point $X = 10\pi$ for $U_0 = 16$, $d = 0.4$, $\psi(x, t = 0) = \chi\varphi_0$ and $\xi = 0.5$. The precursor is made by the contribution of the opposite spin. Other parameters are the same as in Fig.2.

For the weak SO coupling $\xi \gg 1$, where $|\psi_{-1}/\psi_1| \ll 1$, the spin polarization can be calculated as:

$$p_y \approx -\sin\frac{x}{\xi} + 2\cos\frac{x}{\xi}\Im\frac{\psi_{-1}}{\psi_1}. \quad (15)$$

Second term in Eq.(15) can be viewed as a result of a correction to the particle displacement in the form $p_y =$

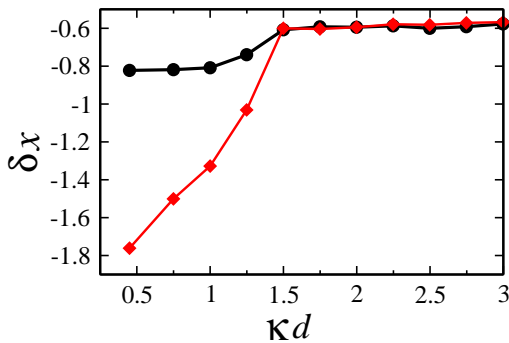


FIG. 7. (Color online) Parameter of additional displacement δx as the function of the barrier transparency. Filled circles correspond to $U_0 = 16$ and variable width d , the squares correspond to $d = 0.4$ with variable U_0 , and $\xi = 10$.

$-\sin(x/\xi + \delta x/\xi)$, where, according to Eqs.(9),(10):

$$\delta x = -2 \lim_{\xi \rightarrow \infty} \xi \Im \frac{\int_0^{\infty} G_{-1}(k) \exp(-ik^2 t/2) \phi_k(x) dk}{\int_0^{\infty} G_1(k) \exp(-ik^2 t/2) \phi_k(x) dk} \quad (16)$$

This deviation of p_y from zero at $X = n\pi\xi$ demonstrates that the real precession angle is $\beta^{[\text{so}]} = \beta_0^{[\text{so}]} + \delta\beta^{[\text{so}]}$, with the correction $\delta\beta^{[\text{so}]}$ can be viewed as a result of additional displacement of the particle δx with $\delta x = \xi\delta\beta^{[\text{so}]}$. From Eq.(16), we can see that δx is independent of the SO coupling, while the parameters of the barrier play an important role, as the eigenfunctions $\phi_k(x)$ strongly depend on them. Numerical results also show that δx is independent of coordinate and time if measured at distance $X \gg a_2$ at times $t > X/v$. The tunneling length δx is presented in Fig.7 for two different barriers. This figure shows a clear crossover from the classical (transparent barrier) to the tunneling (opaque barrier) regimes, where δx shows a saturation, and the additional displacement

is universal. The saturation of the tunneling length for opaque barriers seems similar to the Hartman effect [35] on the group delay in a scattering case [36]. However, after making comparisons of $\delta t \equiv \delta x/v$ and calculated group delay for a single barrier with parameters presented in Fig.7, we cannot draw the unambiguous conclusion on the relevance of these two quantities.

V. CONCLUSIONS

In conclusion, we investigated the spin dynamics of a tunneling particle initially localized in a potential in the presence of SO coupling. It is shown that at short-time scales initial states play an important role in spin polarization while the spin density and probability density possess diffraction-in-time phenomenon at long-time scales. We showed that in addition to the time, tunneling can be characterized by a characteristic length. We use the rotation angle to identify the tunneling length in the presence of weak coupling. The tunneling length depends on the barrier parameters, being independent on the strength of the spin-orbit coupling. These effects can be observed in experiments with cold atoms, where the SO coupling is strong enough to cause spin precession on a relatively short spatial scale.

ACKNOWLEDGEMENT

This work of EYS was supported by the MCINN of Spain Grant FIS2009-12773-C02-01, by ‘‘Grupos Consolidados UPV/EHU del Gobierno Vasco’’ Grant IT-472-10, and by the UPV/EHU under program UFI 11/55. Y. B. acknowledges financial support from the Basque Government (Grant No. BFI-2010-255). We are grateful to J.G. Muga and D. Sokolovski for valuable discussions.

-
- [1] I. Žutić, J. Fabian and S. Das Sarma, Rev. Mod. Phys. **76**, 323 (2004).
 - [2] S. Amasha, K. MacLean, I. P. Radu, D. M. Zumbühl, M. A. Kastner, M. P. Hanson, and A. C. Gossard, Phys. Rev. B **78**, 041306(R) (2008).
 - [3] P. Stano and P. Jacquod, Phys. Rev. B **82**, 125309 (2010).
 - [4] P. Stano and J. Fabian, Phys. Rev. B **72**, 155410 (2005).
 - [5] R. Romo and S. E. Ulloa, Phys. Rev. B **72**, 121305(R) (2005).
 - [6] I. Malajovich, J. M. Kikkawa, and D. D. Awschalom, J.J. Berry and N. Samarth, Phys. Rev. Lett. **84**, 1015 (2000).
 - [7] D. D. Awschalom and M. E. Flatté, Nat. Phys. **3**, 153 (2007).
 - [8] T. D. Stanescu, B. Anderson, and V. Galitski, Phys. Rev. A **78**, 023616 (2008).
 - [9] X.-J. Liu, M. F. Borunda, X. Liu, and J. Sinova, Phys. Rev. Lett. **102**, 046402 (2009).
 - [10] C. Wang, C. Gao, C.-M. Jian, and H. Zhai, Phys. Rev. Lett. **105**, 160403 (2010).
 - [11] Y.-J. Lin, K. Jimenez-Garcia, and I. B. Spielman, Nature **471**, 83 (2011).
 - [12] D. L. Campbell, G. Juzeliūnas, and I. B. Spielman, Phys. Rev. A **84**, 025602 (2011)
 - [13] M. M. Glazov, P. S. Alekseev, M. A. Odnoblyudov, V. M. Chistyakov, S. A. Tarasenko, and I. N. Yassievich, Phys. Rev. B **71**, 155313 (2005).
 - [14] D. Khomitsky and E. Ya. Sherman, EPL **90**, 27010 (2010).
 - [15] X. Zheng, F. Wang, C.-Y. Yam, Y. Mo, and G.H. Chen, Phys. Rev. B **75**, 195127 (2007), Y. Wang, C.-Y. Yam, G.H. Chen, T. Frauenheim, and T.A. Niehaus, Chem. Phys. **391**, 69 (2011), C.-Y. Yam, X. Zheng, G.H. Chen,

- Y. Wang, Th. Frauenheim, and T.A. Niehaus, Phys. Rev. B **83**, 245448 (2011).
- [16] A. Marchewka and E. Granot, Phys. Rev. A **79**, 012106 (2009).
- [17] G. Kälbermann, Phys. Rev. C **79**, 024613 (2009); **77**, 041601 (2008).
- [18] N. G. Kelkar, H.M. Castañeda, and M. Nowakowski, Europhys. Lett. **85**, 20006 (2009).
- [19] S. Cordero, G. García-Calderón, R. Romo, and J. Villavicencio, Phys. Rev. A **84**, 042118 (2011).
- [20] M. Pons, D. Sokolovski, and A. del Campo, Phys. Rev. A **85**, 022107 (2012).
- [21] A. I. Baz', Yad. Fiz. **5**, 229 (1967).
- [22] V. F. Rybachenko, Yad. Fiz. **5**, 895 (1967).
- [23] R. A. Sepkhanov, M. V. Medvedyeva, and C. W. J. Beenakker, Phys. Rev. B **80**, 245433 (2009).
- [24] B. Huang and I. Appelbaum, Phys. Rev. B **82**, 241202(R) (2010).
- [25] M. Büttiker and R. Landauer, Phys. Rev. Lett. **49**, 1739 (1982).
- [26] M. Büttiker, Phys. Rev. B **27**, 6178 (1983).
- [27] V. A. Sablikov and Y. Ya. Tkach, Phys. Rev. B **76**, 245321 (2007).
- [28] V. I. Perel', S. A. Tarasenko, I. N. Yassievich, S. D. Ganichev, V. V. Bel'kov, and W. Prettl, Phys. Rev. B **67**, 201304 (2003).
- [29] Y. Ban, E. Ya. Sherman, J. G. Muga, and M. Büttiker, Phys. Rev. A **82**, 062121 (2010).
- [30] K. Henderson, C. Ryu, C. MacCormick and M. G. Boshie, New J. Phys. **11**, 043030 (2009).
- [31] M. Moshinsky, Phys. Rev. **88**, 625 (1952). The result of this paper can be understood in terms of diffraction of perfectly coherent propagating waves. For decay of a metastable state, the diffraction can be seen as produced by partially coherent waves: M. Born and E. Wolf, *Principles of Optics*, Chapter X, 1999 (7th Ed.), see also in Ref. [34].
- [32] A. Steane, P. Szafrtger, P. Desbiolles, and J. Dalibard, Phys. Rev. Lett. **74**, 4972 (1995).
- [33] A. del Campo, G. García-Calderón, and J.G. Muga, Phys. Rep. **476**, 1 (2009).
- [34] E. Torrontegui, J. Muñoz, Y. Ban, and J. G. Muga, Phys. Rev. A **83**, 043608 (2011).
- [35] T. E. Hartman, J. Appl. Phys. **33**, 3427 (1962).
- [36] E. P. Wigner, Phys. Rev. **98**, 145 (1955).